BRUKER

JPK BIOAFM **Application Note**

Atomic Force Microscopy
Automated Force Spectroscopy
Optical Tweezers/Optical Trapping
Cell/Tissue Mechanics & Cell Adhesion

Correlative AFM and Super-Resolution STED Analysis of DNA Nanostructures

Introduction

In the past decades, atomic force microscopy (AFM) has become standard in the high-resolution structural analysis of samples ranging from single molecules to complex macromolecular systems [1, 2]. Unlike other high-resolution imaging techniques, it does not require any specific sample modification (except for surface deposition), the risk, therefore, of introducing artefacts through sample preparation is reduced. In recent years, there has been an increased demand for and application of novel developments featuring high-speed AFM imaging (>10 frames/sec), quantitative nanomechanical characterization of samples, and advanced feedback imaging modes which tweak the maximum attainable resolution.

Furthermore, the examination of, e.g. specific molecules or features carrying immunochemical information has been made possible by combining AFM with recent developments in optical/fluorescence microscopy, and in doing so, complementing the advantages of both techniques and enabling true correlative microscopy [3].

Correlative and high-speed AFM

The measurements presented here were carried out using the recently launched JPK NanoWizard® ULTRA Speed 2 with the 2nd generation Vortis™ controller (Bruker Nano), a benchmark in correlative, high-speed BioAFM combined with advanced optical microscopy. The system features easy-to-use modes such as QI™, which allows reliable and reproducible imaging of very soft and delicate samples in liquid, as well as the quantification of mechanical and adhesive sample properties with nanometer resolution. More advanced modes such as the HyperDrive™ allow highest resolution imaging of the topography of very small and fragile structures like single molecules in liquid. To conclude, we have demonstrated the capability of the instrument to non-invasively scan DNA nanostructures at 400 lines/s in closed-loop mode.

Fig. 1: *JPK NanoWizard AFM family integrated with a compact line STEDYCON (Abberior Instruments), on an AxioObserver (Zeiss).*

A schematic representation of a typical instrumental setup for the advanced correlative measurements used here is shown below (Fig.1).

STED - a super-resolution microscopy technique

In recent years a variety of super-resolution microscopy techniques have been developed, all proposing different concepts for overcoming the Abbe diffraction limit, which defines the minimum resolvable distance between two point-like objects [4]. The resolution of an optical microscope ends at approx. 200 nm laterally and 600 nm axially. In 1994, Hell and Wichmann developed a unique strategy for breaking the diffraction limit, stimulated emission depletion (STED), which was awarded the Nobel Prize in Chemistry in 2014 [5]. STED microscopy uses two laser pulses, the first one excites and the second one de-excites the fluorophores, fluorescent chemical compounds
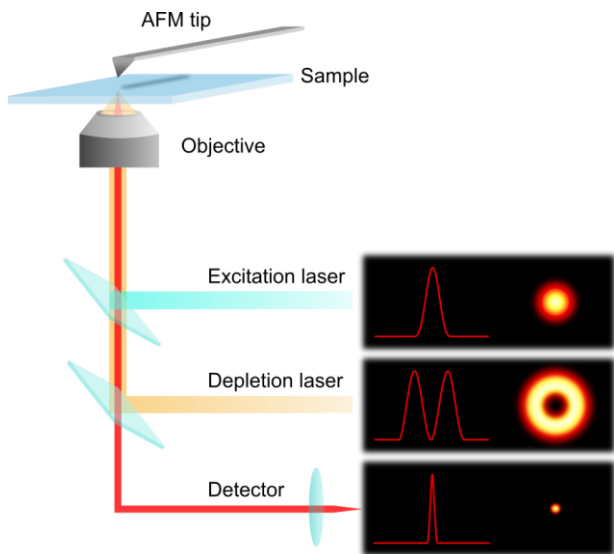
Fig. 2: Principle of combined AFM and STED microscopy. *The "donut" shape of the encircling depletion (STED) laser confines the spot of effective fluorescence*

that can re-emit light upon light excitation. The excitation laser focus scans the sample, whereas the depletion donut-shaped STED beam switches off the fluorophores at the rim of the focal point, thus confining the spot of effective fluorescence (Fig. 2). Increasing the intensity of the STED beam reduces the full width at half maximum (FWHM) of the effective focal spot d_{STED} as shown below:

$$d_{STED} = \lambda / \left(2n \sin \alpha \sqrt{1 + I/I_S} \right)$$

with λ being the wavelength, n - refractive index of the medium, α - the half-aperture angle of the objective, I – depletion STED beam intensity, and I_S – characteristic saturation intensity for a particular fluorophore at which the emitted fluorescence is reduced by a factor of $1/e$.

DNA as a nanoscale building block

Deoxyribonucleic acid (DNA) is a polymer that chemists dream of. Its inherent structure is based on four organic bases that comprises two alpha-helical strands held together by hydrogen bonds [6]. Following a certain complementarity code, the sequences in the strands not only bind to one another, but also create numerous possibilities for (non)-directed self-assembly into intricate shapes and structures on the nanoscale [7]. The sequence of a DNA strand defines the way it assembles, which allows the prediction/modelling of the final structure a DNA molecule will adopt *in vitro*. By using specific sequences, one or several DNA strands can be forced to assemble into complex architectures. Seeman laid the foundation for

exploiting DNA for nanotechnology and described several strategies for the formation of complex DNA structures [8]. The ongoing development of novel design strategies increases the diversity of structures and their applications in many fields. For instance, Ackermann et al. presented rotaxanes made from DNA, opening new possibilities for research into molecular machines and synthetic biology [9, 10]. Benson et al. demonstrated an automated technique for converting digitally generated flat sheet meshes into scaffolded DNA structures [11].
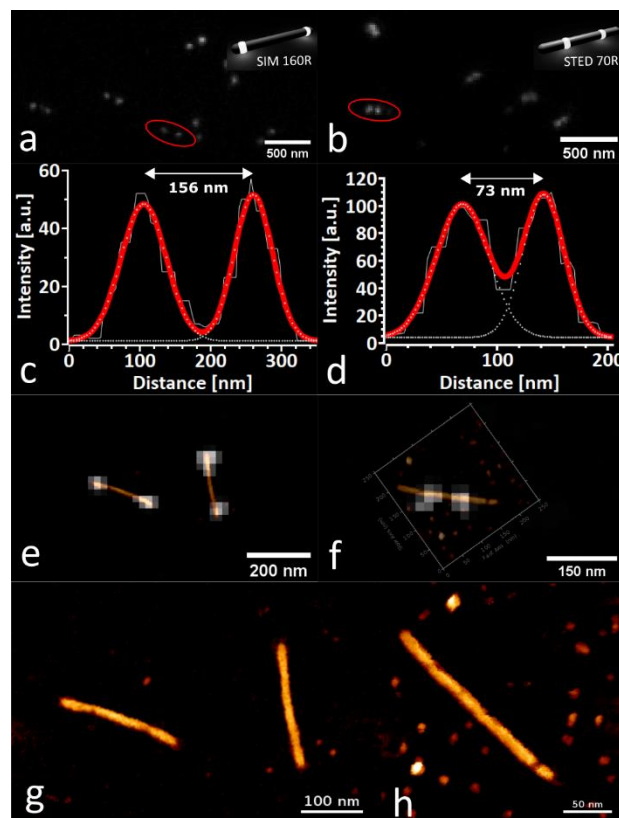
DNA-based nanorulers

Fig. 3: Correlative AFM of DNA Nanorulers. *(a, b) are STED measurements of the corresponding SIM 160R and STED 70R nanorulers, measured in TAE-1x (Mg) buffer. Insets are sketches of GATTAquant nanorulers with different mark-to-mark distances (70-160 nm, both labelled with Atto647N), reproduced with permission from [15]. (c, d) show bi-sigmoidal Gaussian fits of the intensity signal along the signified cross-sections in (a, b). (e, f) Optical correlation of the consecutively acquired STED and AFM images of the DNA nanorulers. (g, h) QI topography channels of the AFM images used for the overlays in (e, f), showing the linearized structure of the DNA nanorulers (z-scale: 10 nm)*

Another application is the use of DNA origami structures as calibration standards for 2D and 3D super-resolution optical microscopes [12–14]. Commercially available DNA-based rulers, used for the quantification and calibration of super-

resolution systems and with a precision of just a few nanometers, are available in different forms with varying fluorophore spacings, fluorescence tags, as well as nanostructure shape and size [15]. To demonstrate the compatibility of such structures for corelative AFM measurements, we used commercially available STED nanorulers (GATTAquant GmbH), which are rod-shaped and modified with dye molecules placed at defined distances along the rod (Fig. 3 a, b).
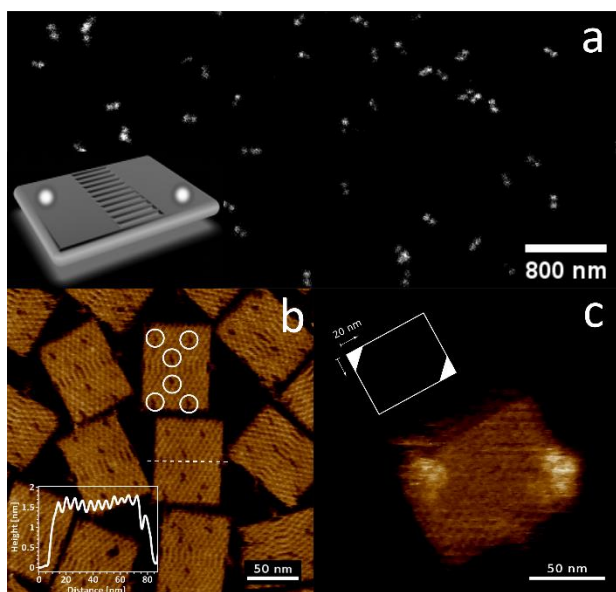
DNA-based origami

Fig. 4: Characterisation of GATTA-AFM rectangular origami. (a-inset) Sketch of a DNA rectangular origami (GATTA-AFM) with the theoretical locations for the Atto647N fluorophores, reproduced with permission from [15]. (a) STED measurement of the corresponding signal from DNA rectangles carrying a fluorophore and measured in TAE-1x (Mg) buffer. (b) Fast amplitude modulation (AM) AFM image of a DNA origami lattice (without a fluorophore) recorded at 10 lines/s. The inset represents a cross-section across the central ladder seam of the DNA nanostructure (Z-scale: 2 nm). (c) Fast phase modulation (PM) AFM image of a DNA origami lattice carrying Atto647N labels, recorded at 10 lines/s. The inset signifies the locations along the lattice which are supposedly carrying the fluorescent tags (Z-scale: 3 nm)

In certain scenarios, it is advantageous to use both an optical and an AFM calibration standard. In this work, we used a new rectangular origami (NRO) design with the dimensions 100 x 70 nm [14]. Such structures are commercially available as GATTA-AFM, in which case they selectively carry two diagonally spaced Atto647N fluorophore populations (Fig. 4a - inset). The STED signal from such structures is shown in Fig. 4a. The molecular substructure of such conformations is easily recognizable in AFM images due to their planar design and two

characteristic hallmarks of their pattern (Fig. 4c). The first is the central ladder seam bridging the crossed halves of the design, which has a pitch of 6 nm, as stated in [15]. Secondly, there are six visible gaps in the NRO lattice (labelled here with circles), which are introduced via shortened staple strands, as designated binding sites for other molecules [14]. The NRO design carrying fluorophores was analysed with phase-modulation AFM (HyperDrive™) and is shown here in Fig. 4c. According to the manufacturer, each binding locus (20 x 20 nm) on the lattice is hybridised by 12-15 ssDNA. These locations are clearly visible at each end, however, due to their length (25 bp), they exhibit a certain hydrodynamic radius fluctuation which prevents a clear resolution of the NRO lattice.

High-speed imaging of DNA origami

High-speed applications are an ongoing development in the repertoire of AFM and have been found to be particularly interesting in the characterization of kinetic and dynamic processes. In the case of DNA origami, such events could be the (non-)assisted self-assembly of surface structures and lattices, or simply the binding of specific single molecules and cargo. Here, we studied the NRO lattices (without fluorophores) with high-speed AFM (Fig. 5).
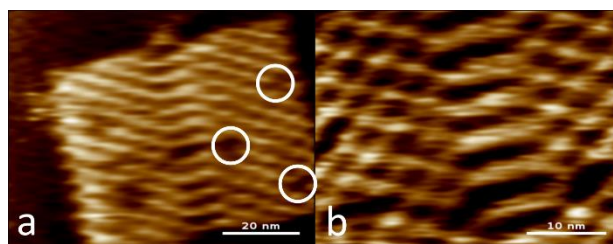

Fig. 5: High-speed AFM images of R80 DNA Origami. Both images (256 x 256 pixels) were recorded at 400 lines/s, resulting in a temporal resolution of ~1.6 frames/s. Z-scale in both images is 2 nm.

The resulting AFM images show that it is possible to non-invasively study the molecular structures of the NRO at a line rate of 400 lines/s and with an image resolution of 256 x 256 pixels. The temporal resolution of 1.6 frames/s (fps) can be further increased to over 10 fps by applying the bi-directional scanning implemented in the NanoWizard ULTRA Speed 2, and/or by scaling down the line resolution. This would in turn make it possible to resolve dynamic events taking place on the millisecond scale.

Conclusion

We have successfully used the latest generation JPK NanoWizard ULTRA Speed 2 AFM to study DNA-based nanostructures with sub-molecular resolution *in vitro*.

Furthermore, it was demonstrated that the instrument can be successfully coupled to a 2D compact line super-resolution STED instrument and can, non-invasively, carry out correlative microscopy with a lateral resolution better than 70 nm. Furthermore, the ability of this setup to study dynamic processes with a temporal resolution of over 1 fps was also demonstrated.

Acknowledgements

Authors

Tanja Neumann, Jörg Barner, Dimitar Stamov (JPK BioAFM Business, Bruker Nano GmbH)

References

1. Stamov DR, Kaemmer SB, Hermsdörfer A, Barner J, Jähnke T, Haschke H (2015) BioScience AFM – Capturing Dynamics from Single Molecules to Living Cells. Microsc Today 23:18–25 . doi: 10.1017/S1551929515001005

2. Winkel AK, Barner J, Henze T, Neumann T, Körnig A, Kumpfe F, Haschke H (2016) The Wide-Open Door: Atomic Force Microscopy 30 Years On. Microsc Today 24:12–17 . doi: 10.1017/S1551929516000900

3. Monserrate A, Casado S, Flors C (2014) Correlative Atomic Force Microscopy and Localization-Based Super-Resolution Microscopy: Revealing Labelling and Image Reconstruction Artefacts. ChemPhysChem 15:647–650 . doi: 10.1002/cphc.201300853

4. Endesfelder U (2018) Super-Resolution Microscopy. A Practical Guide. By Udo J. Birk. Angew Chem Int Ed 57:7939–7939 . doi: 10.1002/anie.201804434

5. Hell SW, Wichmann J (1994) Breaking the diffraction resolution limit by stimulated emission: stimulated-emission-depletion fluorescence microscopy. Opt Lett 19:780–782 . doi: 10.1364/OL.19.000780

6. Watson JD, Crick FHC (1953) Molecular Structure of Nucleic Acids: A Structure for Deoxyribose Nucleic Acid. Nature 171:737–738 . doi: 10.1038/171737a0

7. Sanderson K (2010) Bioengineering: What to make with DNA origami. Nature 464:158–159 . doi: 10.1038/464158a

8. Seeman NC (1998) DNA NANOTECHNOLOGY: Novel DNA Constructions. Annu Rev Biophys Biomol Struct 27:225–248 . doi: 10.1146/annurev.biophys.27.1.225

9. Ackermann D, Schmidt TL, Hannam JS, Purohit CS, Heckel A, Famulok M (2010) A double-stranded DNA rotaxane. Nat Nanotechnol 5:436–442 . doi: 10.1038/nnano.2010.65

10. Ackermann D, Jester S-S, Famulok M (2012) Design Strategy for DNA Rotaxanes with a Mechanically Reinforced PX100 Axle. Angew Chem Int Ed 51:6771–6775 . doi: 10.1002/anie.201202816

11. Benson E, Mohammed A, Bosco A, Teixeira AI, Orponen P, Högberg B (2016) Computer-Aided Production of Scaffolded DNA Nanostructures from Flat Sheet Meshes. Angew Chem Int Ed 55:8869–8872 . doi: 10.1002/anie.201602446

12. Steinhauer C, Jungmann R, Sobey T, Simmel F, Tinnefeld P (2009) DNA Origami as a Nanoscopic Ruler for Super-Resolution Microscopy. Angew Chem Int Ed 48:8870–8873 . doi: 10.1002/anie.200903308

13. Schmied JJ, Forthmann C, Pibiri E, Lalkens B, Nickels P, Liedl T, Tinnefeld P (2013) DNA Origami Nanopillars as Standards for Three-Dimensional Superresolution Microscopy. Nano Lett 13:781–785 . doi: 10.1021/nl304492y

14. Schmied JJ, Raab M, Forthmann C, Pibiri E, Wünsch B, Dammeyer T, Tinnefeld P (2014) DNA origami–based standards for quantitative fluorescence microscopy. Nat Protoc 9:1367–1391 . doi: 10.1038/nprot.2014.079

15. Gattaquant DNA Nanotechnologies. In: Gattaquant DNA Nanotechnologies. http://www.gattaquant.com/. Accessed 28 Jan 2019

JPK BioAFM Business
Bruker Nano GmbH
Am Studio 2D, 12489 Berlin, Germany
productinfo@bruker.com
www.bruker.com/bioafm · www.jpk.com